Journal of the Brazilian Society of Mechanical Sciences and Engineering (2024) 46:218
https://doi.org/10.1007/s40430-024-04721-4

TECHNICAL PAPER

Propagation of Lamb wave in the plate of microstretch thermoelastic diffusion materials

Sanjay Debnath[1] · S. S. Singh[1]

Received: 6 April 2023 / Accepted: 15 January 2024 / Published online: 15 March 2024

Abstract

The present paper investigates the three thermoelastic theories on the propagation of Lamb wave in a linearly isotropic microstretch diffusion plate subjected to the thermally insulated/impermeable and isothermal/isoconcentrated boundary conditions. The secular equations of the Lamb wave are obtained for both symmetric and anti-symmetric modes of vibration. The secular equations for Rayleigh surface wave at short wavelength and plate wave at longer wavelength are obtained for both the boundary conditions from symmetric vibration. We also obtain the secular equation of flexural wave from the anti-symmetric vibration at the longer wavelength compared with the thickness of the plates. The phase velocity and attenuation are computed numerically for a particular model, and these results are compared for the coupled themoelasticity(CT), Lord–Shulman ($L-S$) and Green–Lindsay ($G-L$) theories. There are three modes of dispersion and attenuation for each symmetric and anti-symmetric vibration. The dispersion curves of the Lamb wave increase from first to third mode of symmetric vibration in both thermally insulated/impermeable and isothermal/isoconcentrated plates. Certain special cases are reduced from the current formulation.

Keywords Microstretch · Thermoelastic theory · Symmetric vibration · Anti-symmetric vibration · Secular equation · Lamb wave

1 Introduction

The theory of micro-continuum explains the complexities lying in the microstructures and discusses the microscopic motion and long-range material interactions. Eringen [1] was perhaps the first who introduced the theory of micromorphic bodies. Eringen [2] also generalized the theory of micropolar elastic materials to develop the theory of microstretch elastic solids. The material points in the microstretch bodies have seven degrees of freedom and can independently stretch and contract along with translations and rotations.

The thermoelastic theory studies the consequences of the disturbances occurred due to thermal, stress and strain fields on an elastic body. Biot [3] presented an unified treatment of thermoelasticity by employing and further developing the method of irreversible thermodynamics using two vector fields, displacement and an entropy flowfield to describe the state of the materials. Lord and Shulman [4] and Green and Lindsay [5] generalized the theory of thermoelasticity that allows finite velocity of transmission for the thermal waves. They introduce one and two thermal relaxation times, respectively, to discuss the thermal character in the continuum body. The theory of thermo-microstretch elastic solid was developed by Eringen [6] to induce the consequences of heat conduction in the microstretch theory and established the uniqueness theorem for the mixed initial boundary value problem. De Cicco and Nappa [7] verified finite velocities for thermal waves in the linearized theory of thermo-microstretch elastic solids. Ciarletta and Scalia [8] studied the spatial and temporal response of thermoelastodynamic phenomenon on microstretch continuum materials.

Sherief et al. [9] proved the variation theorem and uniqueness of the governing equations for the generalized thermoelastic diffusion materials. Aouadi [10] derived the equations of generalized thermoelastic diffusion, based on the

Technical Editor: Aurelio Araujo.

✉ S. S. Singh
saratcha32@yahoo.co.uk

Sanjay Debnath
sdnath613@gmail.com

[1] Department of Mathematics & Computer Science, Mizoram University, Aizawl, Mizoram 796 004, India

Lord–Shulman theory and established the uniqueness and reciprocity theorem using Laplace transformation. Aouadi [11] inferred the field equations for thermoelastic diffusion plates considering three distinct heat and diffusion transmission laws. Khurana and Tomar [12] established the existence of three longitudinal and two transverse frequency dependent waves in non-local microstretch solid. Goyal et al. [13] investigated the inhomogeneous nature of Rayleigh waves with the aid of its secular equations in a swelling porous medium. Kumar [14] presented the characteristics of harmonic waves traveling through thermo-microstretch diffusion medium and obtained the amplitude/energy ratios of the reflected and refracted waves. Kumar et al. [15] developed the dispersion relations for Rayleigh waves through microstretch thermoelastic diffusion medium under a liquid layer with negligible viscosity. Singh et al. [16] derived the reflection and refraction coefficients in microstretch thermoelastic diffusion half-spaces subject to three distinct thermoelastic theories. Royer and Dieulesaint [17] summarized the theories related to the propagation of elastic waves in different materials, wave equations and their solutions, energy flow and reflection/refraction phenomena. Some important problems in thermoelastic materials are Singh [18], Zorammuana and Singh [19], Singh and Lianngenga [20], Lotfy and Othman [21], Singh and Tochhawng [22], Kumar and Kansal [23], Abo-Dahab et al. [24], Kumar et al.[25, 26], Singh and Yadav [27].

Lamb [28] examined surface waves in an isotropic elastic plate where the wave moves parallel to the medial plane. Zhu and Wu [29] obtained the dispersion equations of Lamb waves of a plate bordered with viscous liquid layer/a half-space of viscous liquid on both sides and evaluated the numerical solutions of dispersion equations. Conry et al. [30] solved the problem of low frequency Rayleigh-Lamb waves and detected the defects/cracks in a centrally embedded aluminum plate. Tomar [31] simulated the frequency equation of Rayleigh-Lamb wave propagation in a plate of micropolar elastic material with voids of finite thickness for velocity and attenuated curves. Lianngenga and Singh [32] studied the problem of symmetric and anti-symmetric vibrations in micropolar thermoelastic plate with voids and obtained the dispersive frequency equations for different surface waves propagating in the plate. We have observed interesting problems of Lamb waves in Sharma and Pal [33], Kumar et al. [34], Kumar and Pratap [35, 36], Sharma and Thakur [37], Sharma and Othman [38], Sharma and Kumar [39], Apostol [40], Ezzin et al. [41], Sharma and Kumar [42] and Goldstein and Kuznetsov [43].

The problems of Lamb wave are frequently used in civil engineering, architectures, navigation, chemical pipes, aerospace engineering, etc. The interest of researchers in such studies are increasing due to its ability to completely understand the structure of plates and shells, which are using in multi-sensors to detect the damages in metallic structures [44], and it is used in health monitoring devices [45, 46]. Our study of Lamb wave in microstretch thermoelastic diffusion plates may give new light to explore the skull and the human brain with better ultrasound imaging system [47, 48]. This investigation may provide to the researchers with an appropriate data to construct new medical and engineering devices. We will compare the results of Lamb wave propagating through a microstretch thermoelastic diffusion plate for the three thermoelastic theories, i.e., *GL*, *LS* and *CT* theories. The secular equations for symmetric and anti-symmetric Lamb wave modes will be derived for stress-free thermally insulated/impermeable and isothermal/isoconcentrated conditions.

2 Governing equations

The equations of motion for linearly isotropic and homogeneous microstretch thermoelastic diffusion media in the absence of body forces and heat sources are given by [2, 9]:

$$\begin{aligned}&(\lambda+2\mu+\kappa)\nabla(\nabla\cdot\mathbf{u})-(\mu+\kappa)\nabla\times\nabla\times\mathbf{u}+\kappa\nabla\times\boldsymbol{\phi}\\&\quad+\lambda_0\nabla\varphi^*-\beta_1(1+\tau_1\frac{\partial}{\partial t})\nabla T-\beta_2(1+\tau^1\frac{\partial}{\partial t})\nabla C\\&\quad=\rho\frac{\partial^2\mathbf{u}}{\partial t^2},\end{aligned}\tag{1}$$

$$\begin{aligned}&(\alpha+\beta+\gamma)\nabla(\nabla\cdot\boldsymbol{\phi})-\gamma\nabla\times\nabla\times\boldsymbol{\phi}+\kappa\nabla\times\mathbf{u}-2\kappa\boldsymbol{\phi}\\&\quad=\rho j\frac{\partial^2\boldsymbol{\phi}}{\partial t^2},\end{aligned}\tag{2}$$

$$\begin{aligned}&\alpha_0\nabla^2\varphi^*+\nu_1\Big(1+\tau_1\frac{\partial}{\partial t}\Big)T+\nu_2\Big(1+\tau^1\frac{\partial}{\partial t}\Big)C\\&\quad-\lambda_1\varphi^*-\lambda_0\nabla\cdot\mathbf{u}=\frac{\rho j_0}{2}\frac{\partial^2\varphi^*}{\partial t^2},\end{aligned}\tag{3}$$

$$\begin{aligned}&\beta_1T_0\Big(1+\varepsilon\tau_0\frac{\partial}{\partial t}\Big)\nabla\cdot\frac{\partial\mathbf{u}}{\partial t}+\nu_1T_0\Big(1+\varepsilon\tau_0\frac{\partial}{\partial t}\Big)\frac{\partial\varphi^*}{\partial t}\\&\quad+\rho C^*\Big(1+\tau_0\frac{\partial}{\partial t}\Big)\frac{\partial T}{\partial t}+aT_0\Big(1+\gamma_1\frac{\partial}{\partial t}\Big)\frac{\partial C}{\partial t}=K^*\nabla^2T,\end{aligned}\tag{4}$$

$$\begin{aligned}&d\beta_2\nabla^2(\nabla\cdot\mathbf{u})+d\nu_2\nabla^2\varphi^*+da\Big(1+\tau_1\frac{\partial}{\partial t}\Big)\nabla^2T\\&\quad+\Big(1+\varepsilon\tau^0\frac{\partial}{\partial t}\Big)\frac{\partial C}{\partial t}-db\Big(1+\tau^1\frac{\partial}{\partial t}\Big)\nabla^2C=0.\end{aligned}\tag{5}$$

Table 1 Nomenclature

Symbols		Symbols	
t_{ij}	Stress tensor	m_{ij}	Couple stress tensor
λ_i^*	Microstress tensor	d	Thermoelastic diffusion constant
$\boldsymbol{\phi}$	Microrotation vector	φ^*	Microstretch scalar function
e_{ij}	Strain tensor	$\alpha, \kappa, \gamma, \beta$	Micropolarity parameters
k	Wavenumber	μ,λ,	Lamé parameters
$T,\ T_0$	Temperature	C	Concentration
e_{ijk}	Alternating symbol	$\lambda_1, \alpha_0, \lambda_0, b_0$	Microstretch parameters
ρ	Density	K^*	Thermal conductivity
C^*	Specific heat	a	Thermoelastic diffusion
$\mathbf{u}$	Displacement	$\alpha_{c1},\ \alpha_{c2}$	Linear diffusion expansion
v	Phase velocity	b	Coefficient of mass diffusion
$j,\ j_0$	Microinertia	τ_1, τ_0	Relaxation times for thermal signals
δ_{ij}	Kronecker delta	τ^1, τ^0	Relaxation times for diffusion signals
ω	Angular velocity	$\alpha_{t1},\ \alpha_{t2}$	Coefficients of linear thermal expansion

The constitutive relations for the linearly isotropic and homogeneous microstretch thermoelastic diffusion solid are given as:

$$t_{ij} = \lambda u_{i,i}\delta_{ij} + 2\mu e_{ij} + \kappa(u_{j,i} - e_{ijk}\phi_k) + \lambda_0\delta_{ij}\varphi^* - \beta_1\left(1 + \tau_1\frac{\partial}{\partial t}\right)T\delta_{ij} - \beta_2\left(1 + \tau^1\frac{\partial}{\partial t}\right)C\delta_{ij}, \tag{6}$$

$$m_{ij} = \alpha\phi_{i,i}\delta_{ij} + \beta\phi_{i,j} + \gamma\phi_{j,i} + b_0 e_{kji}\varphi^*_{,k}, \quad \lambda_i^* = \alpha_0\varphi^*_{,i} + b_0 e_{ijk}\phi_{j,k}, \tag{7}$$

Here, $\beta_1 = (3\lambda + 2\mu + \kappa)\alpha_{t1}$, $\beta_2 = (3\lambda + 2\mu + \kappa)\alpha_{c1}$, $\nu_1 = (3\lambda + 2\mu + \kappa)\alpha_{t2}$, $\nu_2 = (3\lambda + 2\mu + \kappa)\alpha_{c2}$ and all the parameters are defined in the Table 1 as nomenclature. The relaxation times are taken in such a way that they satisfy $\tau^1 \geq \tau^0 \geq 0$ and $\tau_1 \geq \tau_0 \geq 0$.

3 Problem formulation and solution

A plate of $2D$ thick microstretch thermoelastic diffusion with initial uniform temperature, T_0 , is considered for the present model. The Cartesian co-ordinate system is taken in such a way that the x_3-axis lies normal to the plate, the $x_1 - x_2$ plane concurs with the middle surface and all three axes intersect at the center of the plate. The plate has free surfaces at $x_3 = \pm D$. Figure 1 provides the outlook geometry of the problem. Take $\mathbf{u} = (u_1, 0, u_3)$ and $\boldsymbol{\phi} = (0, \phi_2, 0)$ for the two-dimensional problem. We introduce the potentials Ω and Ω' for $\mathbf{u}$ so that

$$u_1 = \frac{\partial\Omega}{\partial x_1} - \frac{\partial\Omega'}{\partial x_3}, \qquad u_3 = \frac{\partial\Omega}{\partial x_3} + \frac{\partial\Omega'}{\partial x_1}. \tag{8}$$

Inserting Eq. (8) into (1–5), we get the following sets of equations

$$(\lambda + 2\mu + \kappa)\nabla^2\Omega + \lambda_0\varphi^* - \beta_1\left(1 + \tau_1\frac{\partial}{\partial t}\right)T - \beta_2\left(1 + \tau^1\frac{\partial}{\partial t}\right)C = \rho\frac{\partial^2\Omega}{\partial t^2}, \tag{9}$$

$$-\lambda_0\nabla^2\Omega + (\alpha_0\nabla^2 - \lambda_1)\varphi^* + \nu_1\left(1 + \tau_1\frac{\partial}{\partial t}\right)T + \nu_2\left(1 + \tau^1\frac{\partial}{\partial t}\right)C = \frac{\rho j_0}{2}\frac{\partial^2\varphi^*}{\partial t^2}, \tag{10}$$

$$\beta_1 T_0\left(1 + \varepsilon\tau_0\frac{\partial}{\partial t}\right)\nabla^2\frac{\partial\Omega}{\partial t} + \nu_1 T_0\left(1 + \varepsilon\tau_0\frac{\partial}{\partial t}\right)\frac{\partial\varphi^*}{\partial t} + \rho C^*\left(1 + \tau_0\frac{\partial}{\partial t}\right)\frac{\partial T}{\partial t} - K^*\nabla^2 T + aT_0\left(1 + \gamma_1\frac{\partial}{\partial t}\right)\frac{\partial C}{\partial t} = 0, \tag{11}$$

$$d\beta_2\nabla^4\Omega + d\nu_2\nabla^2\varphi^* + da\left(1 + \tau_1\frac{\partial}{\partial t}\right)\nabla^2 T + \left(1 + \varepsilon\tau^0\frac{\partial}{\partial t}\right)\frac{\partial C}{\partial t} - db\left(1 + \tau^1\frac{\partial}{\partial t}\right)\nabla^2 C = 0, \tag{12}$$

$$(\mu + \kappa)\nabla^2\Omega' + \kappa\phi_2 = \rho\frac{\partial^2\Omega'}{\partial t^2}, \quad -\kappa\nabla^2\Omega' + (\gamma\nabla^2 - 2\kappa)\phi_2 = \rho j\frac{\partial^2\phi_2}{\partial t^2}. \tag{13}$$

Equations (9–12) show four coupled longitudinal waves in Ω, φ^*, T and C, while Eq. (13) gives two coupled shear waves in Ω' and ϕ_2.

For the plane waves propagating along x_1-axis, the following form of solution is taken as:

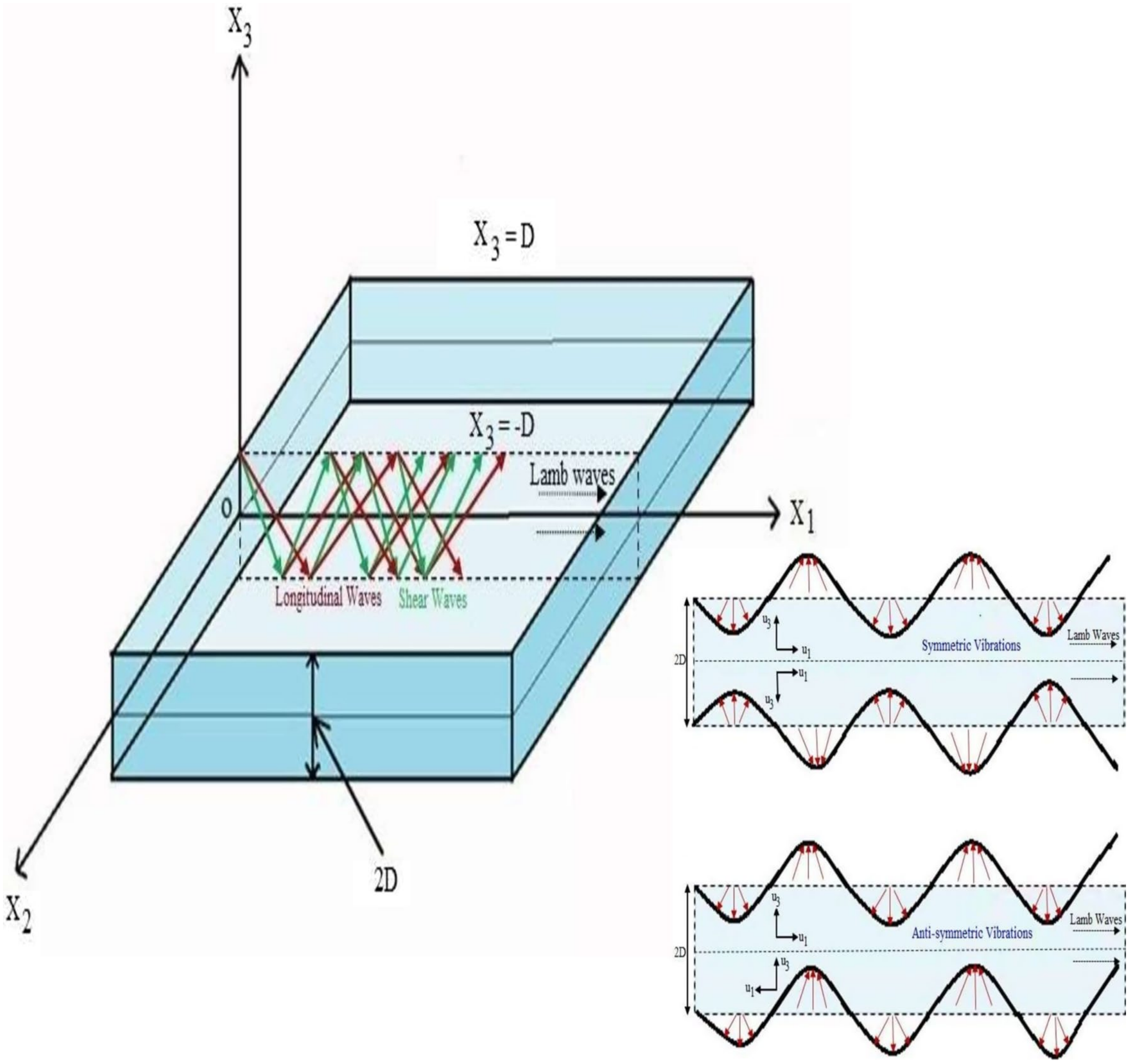

Fig. 1 Geometry of the problem

$$\left\{\Omega, T, \varphi^*, C, \Omega', \phi_2\right\}(x_1, x_3, t) = \left\{\overline{\Omega}, \overline{T}, \overline{\varphi^*}, \overline{C}, \overline{\Omega}', \overline{\phi}_2\right\}(x_3)e^{\iota k(x_1 - vt)}, \tag{14}$$

where $\overline{\Omega}$, $\overline{\varphi^*}$, $\overline{C}$, $\overline{T}$, $\overline{\Omega}'$ and $\overline{\phi}_2$ are the functions of x_3, $\omega(= kv)$ is the angular frequency, k is the wavenumber and v is the phase velocity.

Inserting Eq. (14) into Eqs. (9–13), we obtain the following solution:

$$\{\Omega, T, \varphi^*, C\}(x_1, x_3, t) = \sum_{i=1}^{4}\{1, \gamma_{1i}, \gamma_{2i}, \gamma_{3i}\}[A_i \cosh(m_i x_3) + B_i \sinh(m_i x_3)]e^{\{\iota k(x_1 - vt)\}}, \tag{15}$$

$$\{\Omega', \phi_2\}(x_1, x_3, t) = \sum_{i=5}^{6}\{1, \gamma_{4i}\}[A_i \sinh(m_i x_3) + B_i \cosh(m_i x_3)]e^{\{\iota k(x_1 - vt)\}}, \tag{16}$$

where A_i and B_i are the unknown amplitudes, m_i for $i = 1, 2, 3, 4$ and $i = 5, 6$ are, respectively, solutions of the following equations

$$A(m^2 - k^2)^4 + B(m^2 - k^2)^3 + C(m^2 - k^2)^2 + E(m^2 - k^2) - F = 0, \tag{17}$$

$$L(m^2 - k^2)^2 + M(m^2 - k^2) - N = 0, \tag{18}$$

where the coefficients A, B, C, E, F, L, M and N are given in Annexure-I. The coupling parameters γ_{1i}, γ_{2i}, γ_{3i} and γ_{4i} are written as:

$$\gamma_{ri} = \frac{P_{ri}}{P_i}, \quad (r = 1,2,3; i = 1,2,3,4) \quad \text{and}$$
$$\gamma_{4i} = \frac{c_{21}^2(m_i^2 - k^2)}{c_{22}^2(m_i^2 - k^2) - c_{23}^2}, \quad (i = 5,6) \tag{19}$$

where the expressions of P_{ri} and P_i are given in Annexure-II.

4 Boundary conditions

We consider two types of thermal and diffusion boundary conditions for the stress-free plate. At $x_3 = \pm D$, these conditions can be written as:

$$t_{x_3x_3} = 0, \quad t_{x_3x_1} = 0, \quad m_{x_3x_2} = 0, \quad \lambda^*_{x_3} = 0, \quad \frac{\partial T}{\partial x_3} + h_1 T = 0,$$
$$\frac{\partial C}{\partial x_3} + h_2 C = 0, \tag{20}$$

where $h_1, h_2 \to 0$ stands for thermally insulated and impermeable boundary, while $h_1, h_2 \to \infty$ stands for isothermal and isoconcentrated boundary.

Using Eqs. (6) and (7) into (20), we have

$$(\lambda + 2\mu + \kappa)\frac{\partial^2 \Omega}{\partial x_3^2} + (2\mu + \kappa)\frac{\partial^2 \Omega'}{\partial x_1 \partial x_3} + \lambda \frac{\partial^2 \Omega}{\partial x_1^2}$$
$$+ \lambda_0 \varphi^* - \beta_1\left(1 + \tau_1 \frac{\partial}{\partial t}\right)T - \beta_2\left(1 + \tau^1 \frac{\partial}{\partial t}\right)C = 0, \tag{21}$$

$$(2\mu + \kappa)\frac{\partial^2 \Omega}{\partial x_1 \partial x_3} - (\mu + \kappa)\frac{\partial^2 \Omega'}{\partial x_3^2} + \mu \frac{\partial^2 \Omega'}{\partial x_1^2} - \kappa \phi_2 = 0, \tag{22}$$

$$\gamma \frac{\partial \phi_2}{\partial x_3} + b_0 \frac{\partial \varphi^*}{\partial x_1} = 0, \quad \alpha_0 \frac{\partial \varphi^*}{\partial x_3} - b_0 \frac{\partial \phi_2}{\partial x_1} = 0. \tag{23}$$

Using Eqs. (15) and (16) into the boundary conditions, we get

$$\sum_{i=1}^{6} a_{1i}[A_i \cosh(m_i D) \pm B_i \sinh(m_i D)] = 0,$$
$$\sum_{i=1}^{6} a_{2i}[A_i \sinh(m_i D) \pm B_i \cosh(m_i D)] = 0, \tag{24}$$

$$\sum_{i=1}^{6} a_{3i}[A_i \cosh(m_i D) \pm B_i \sinh(m_i D)] = 0,$$
$$\sum_{i=1}^{6} a_{4i}[A_i \sinh(m_i D) \pm B_i \cosh(m_i D)] = 0, \tag{25}$$

(for thermally insulated and impermeable boundary)

$$\sum_{i=1}^{6} a_{5i}[A_i \sinh(m_i D) \pm B_i \cosh(m_i D)] = 0,$$
$$\sum_{i=1}^{6} a_{6i}[A_i \sinh(m_i D) \pm B_i \cosh(m_i D)] = 0, \tag{26}$$

(for isothermal and isoconcentrated boundary)

$$\sum_{i=1}^{6} a_{7i}[A_i \cosh(m_i D) \pm B_i \sinh(m_i D)] = 0,$$
$$\sum_{i=1}^{6} a_{8i}[A_i \cosh(m_i D) \pm B_i \sinh(m_i D)] = 0. \tag{27}$$

where the nonzero a_{ji} are given by:

$$a_{1i} = (\lambda + 2\mu + \kappa)m_i^2 - \lambda k^2 + \lambda_0 \gamma_{2i} - \beta_1(1 - \iota\tau_1\omega)\gamma_{1i}$$
$$- \beta_2(1 - \iota\tau^1\omega)\gamma_{3i}, \quad a_{2i} = (\kappa + 2\mu)\iota k m_i,$$
$$a_{3i} = \iota b_0 k \gamma_{2i}, \quad a_{4i} = \alpha_0 m_i \gamma_{2i}, \quad a_{5i} = \gamma_{1i} m_i, \quad a_{6i} = \gamma_{3i} m_i, \quad a_{7i} = \gamma_{1i},$$
$$a_{8i} = \gamma_{3i}, \quad i = 1,2,3,4$$
$$a_{1i} = (\kappa + 2\mu)\iota k m_i, \quad a_{2i} = -[(\mu + \kappa)m_i^2 + \mu k^2 + \kappa \gamma_{4i}],$$
$$a_{3i} = \gamma m_i \gamma_{4i}, \quad a_{4i} = -\iota b_0 k \gamma_{4i}, \quad i = 5,6.$$

5 Secular equation

5.1 For thermally insulated and impermeable boundary

We separate A_i and B_i in Eqs. (24–26) by adding and subtracting two suitable equations of the system and obtain the following two set of equations as

$$\begin{pmatrix} a_{11}C_{h1} & a_{12}C_{h2} & a_{13}C_{h3} & a_{14}C_{h4} & a_{15}C_{h5} & a_{16}C_{h6} \\ a_{21}S_{h1} & a_{22}S_{h2} & a_{23}S_{h3} & a_{24}S_{h4} & a_{25}S_{h5} & a_{26}S_{h6} \\ a_{31}C_{h1} & a_{32}C_{h2} & a_{33}C_{h3} & a_{34}C_{h4} & a_{35}C_{h5} & a_{36}C_{h6} \\ a_{41}S_{h1} & a_{42}S_{h2} & a_{43}S_{h3} & a_{44}S_{h4} & a_{45}S_{h5} & a_{46}S_{h6} \\ a_{51}S_{h1} & a_{52}S_{h2} & a_{53}S_{h3} & a_{54}S_{h4} & 0 & 0 \\ a_{61}S_{h1} & a_{62}S_{h2} & a_{63}S_{h3} & a_{64}S_{h4} & 0 & 0 \end{pmatrix} \begin{pmatrix} A_1 \\ A_2 \\ A_3 \\ A_4 \\ A_5 \\ A_6 \end{pmatrix} = 0, \tag{28}$$

$$\begin{pmatrix} a_{11}S_{h1} & a_{12}S_{h2} & a_{13}S_{h3} & a_{14}S_{h4} & a_{15}S_{h5} & a_{16}S_{h6} \\ a_{21}C_{h1} & a_{22}C_{h2} & a_{23}C_{h3} & a_{24}C_{h4} & a_{25}C_{h5} & a_{26}C_{h6} \\ a_{31}S_{h1} & a_{32}S_{h2} & a_{33}S_{h3} & a_{34}S_{h4} & a_{35}S_{h5} & a_{36}S_{h6} \\ a_{41}C_{h1} & a_{42}C_{h2} & a_{43}C_{h3} & a_{44}C_{h4} & a_{45}C_{h5} & a_{46}C_{h6} \\ a_{51}C_{h1} & a_{52}C_{h2} & a_{53}C_{h3} & a_{54}C_{h4} & 0 & 0 \\ a_{61}C_{h1} & a_{62}C_{h2} & a_{63}C_{h3} & a_{64}C_{h4} & 0 & 0 \end{pmatrix} \begin{pmatrix} B_1 \\ B_2 \\ B_3 \\ B_4 \\ B_5 \\ B_6 \end{pmatrix} = 0, \tag{29}$$

where $C_{hi} = \cosh(m_i D)$, $S_{hi} = \sinh(m_i D)$.

The non-trivial solution of Eqs. (28) and (29) gives the secular equations for the symmetric and anti-symmetric modes of vibrations, respectively, as

$$
\begin{aligned}
&a_{1231}a'_{3456}c_{t12}+a_{1133}a'_{2456}c_{t13}+a_{1431}a'_{2356}c_{t14}+a_{1135}a'_{2346}c_{t15}+a_{1631}a'_{2345}c_{t16}\\
&+a_{1332}a'_{1456}c_{t23}+a_{1234}a'_{1356}c_{t24}+a_{1532}a'_{1346}c_{t25}+a_{1236}a'_{1345}c_{t26}+a_{1433}a'_{1256}c_{t34}\\
&+a_{1335}a'_{1246}c_{t35}+a_{1633}a'_{1245}c_{t36}+a_{1534}a'_{1236}c_{t45}+a_{1436}a'_{1235}c_{t46}+a_{1635}a'_{1234}c_{t56}=0,
\end{aligned}
\tag{30}
$$

and

$$
\begin{aligned}
&a_{1231}a'_{3456}t_{12}+a_{1133}a'_{2456}t_{13}+a_{1431}a'_{2356}t_{14}+a_{1135}a'_{2346}t_{15}+a_{1631}a'_{2345}t_{16}\\
&+a_{1332}a'_{1456}t_{23}+a_{1234}a'_{1356}t_{24}+a_{1532}a'_{1346}t_{25}+a_{1236}a'_{1345}t_{26}+a_{1433}a'_{1256}t_{34}\\
&+a_{1335}a'_{1246}t_{35}+a_{1633}a'_{1245}t_{36}+a_{1534}a'_{1236}t_{45}+a_{1436}a'_{1235}t_{46}+a_{1635}a'_{1234}t_{56}=0,
\end{aligned}
\tag{31}
$$

where

$$a_{ijkl}=a_{ij}a_{kl}-a_{il}a_{kj},\quad c_{tij}=\coth(m_iD)\coth(m_jD),\quad t_{ij}=\tanh(m_iD)\tanh(m_jD),$$

$$a'_{pqrs}=\begin{vmatrix} a_{2p} & a_{2q} & a_{2r} & a_{2s}\\ a_{4p} & a_{4q} & a_{4r} & a_{4s}\\ a_{5p} & a_{5q} & a_{5r} & a_{5s}\\ a_{6p} & a_{6q} & a_{6r} & a_{6s}\end{vmatrix}\ \text{for}\ i,j,k,l,p,q,r,s=1(1)6\ \text{and for}\ s,r\geq 5,\ a_{jr}=a_{js}=0,\ j=5,6.$$

5.2 For isothermal and isoconcentrated boundary

Using Eqs. (24), (25) and (27), we obtain the following two set of equations as

$$
\begin{pmatrix}
a_{11}C_{h1} & a_{12}C_{h2} & a_{13}C_{h3} & a_{14}C_{h4} & a_{15}C_{h5} & a_{16}C_{h6}\\
a_{21}S_{h1} & a_{22}S_{h2} & a_{23}S_{h3} & a_{24}S_{h4} & a_{25}S_{h5} & a_{26}S_{h6}\\
a_{31}C_{h1} & a_{32}C_{h2} & a_{33}C_{h3} & a_{34}C_{h4} & a_{35}C_{h5} & a_{36}C_{h6}\\
a_{41}S_{h1} & a_{42}S_{h2} & a_{43}S_{h3} & a_{44}S_{h4} & a_{45}S_{h5} & a_{46}S_{h6}\\
a_{71}C_{h1} & a_{72}C_{h2} & a_{73}C_{h3} & a_{74}C_{h4} & 0 & 0\\
a_{81}C_{h1} & a_{82}C_{h2} & a_{83}C_{h3} & a_{84}C_{h4} & 0 & 0
\end{pmatrix}
\begin{pmatrix} A_1\\ A_2\\ A_3\\ A_4\\ A_5\\ A_6\end{pmatrix}=0,
\tag{32}
$$

$$
\begin{pmatrix}
a_{11}S_{h1} & a_{12}S_{h2} & a_{13}S_{h3} & a_{14}S_{h4} & a_{15}S_{h5} & a_{16}S_{h6}\\
a_{21}C_{h1} & a_{22}C_{h2} & a_{23}C_{h3} & a_{24}C_{h4} & a_{25}C_{h5} & a_{26}C_{h6}\\
a_{31}S_{h1} & a_{32}S_{h2} & a_{33}S_{h3} & a_{34}S_{h4} & a_{35}S_{h5} & a_{36}S_{h6}\\
a_{41}C_{h1} & a_{42}C_{h2} & a_{43}C_{h3} & a_{44}C_{h4} & a_{45}C_{h5} & a_{46}C_{h6}\\
a_{71}S_{h1} & a_{72}S_{h2} & a_{73}S_{h3} & a_{74}S_{h4} & 0 & 0\\
a_{81}S_{h1} & a_{82}S_{h2} & a_{83}S_{h3} & a_{84}S_{h4} & 0 & 0
\end{pmatrix}
\begin{pmatrix} B_1\\ B_2\\ B_3\\ B_4\\ B_5\\ B_6\end{pmatrix}=0,
\tag{33}
$$

The non-trivial solution of Eqs. (32) and (33) gives the secular equation for the symmetric and anti-symmetric modes of vibrations, respectively, as

$$
\begin{aligned}
&a_{2241}a''_{3456}t_{12}+a_{2143}a''_{2456}t_{13}+a_{2441}a''_{2356}t_{14}+a_{2145}a''_{2346}t_{15}+a_{2641}a''_{2345}t_{16}\\
&+a_{2342}a''_{1456}t_{23}+a_{2244}a''_{1356}t_{24}+a_{2542}a''_{1346}t_{25}+a_{2246}a''_{1345}t_{26}+a_{2443}a''_{1256}t_{34}\\
&+a_{2345}a''_{1246}t_{35}+a_{2643}a''_{1245}t_{36}+a_{2544}a''_{1236}t_{45}+a_{2446}a''_{1235}t_{46}+a_{2645}a''_{1234}t_{56}=0,
\end{aligned}
\tag{34}
$$

and

$$
\begin{aligned}
&a_{2241}a''_{3456}c_{t12}+a_{2143}a''_{2456}c_{t13}+a_{2441}a''_{2356}c_{t14}+a_{2145}a''_{2346}c_{t15}+a_{2641}a''_{2345}c_{t16}\\
&+a_{2342}a''_{1456}c_{t23}+a_{2244}a''_{1356}c_{t24}+a_{2542}a''_{1346}c_{t25}+a_{2246}a''_{1345}c_{t26}+a_{2443}a''_{1256}c_{t34}\\
&+a_{2345}a''_{1246}c_{t35}+a_{2643}a''_{1245}c_{t36}+a_{2544}a''_{1236}c_{t45}+a_{2446}a''_{1235}c_{t46}+a_{2645}a''_{1234}c_{t56}=0,
\end{aligned}
\tag{35}
$$

where

$$a''_{pqrs} = \begin{vmatrix} a_{1p} & a_{1q} & a_{1r} & a_{1s} \\ a_{3p} & a_{3q} & a_{3r} & a_{3s} \\ a_{7p} & a_{7q} & a_{7r} & a_{7s} \\ a_{8p} & a_{8q} & a_{8r} & a_{8s} \end{vmatrix} \quad \text{for } p,q,r,s = 1(1)6 \text{ and for } s,r \geq 5, \; a_{jr} = a_{js} = 0, \; j = 7,8.$$

These secular equations are transcendental by nature and contain complete information about the phase velocity, wavenumber and attenuation of the surface waves. Since the wavenumbers are complex quantities, these waves are attenuated.

6 Limiting cases

6.1 Symmetric vibration

We obtain the secular equation for plate wave when the wavelength is longer compared to the thickness $2D$. The quantity kD is small, and hence, m_iD is also small as long as the velocity of the surface wave is finite. In such case, $\tanh x \to x$. Equations (30) and (34), respectively, reduce to

$$\begin{aligned} &a_{1231}a'_{3456}m_{3456} + a_{1133}a'_{2456}m_{2456} + a_{1431}a'_{2356}m_{2356} + a_{1135}a'_{2346}m_{2346} + a_{1631}a'_{2345}m_{2345} + \\ &a_{1332}a'_{1456}m_{1456} + a_{1234}a'_{1356}m_{1356} + a_{1532}a'_{1346}m_{1346} + a_{1236}a'_{1345}m_{1345} + a_{1433}a'_{1256}m_{1256} + \\ &a_{1335}a'_{1246}m_{1246} + a_{1633}a'_{1245}m_{1245} + a_{1534}a'_{1236}m_{1236} + a_{1436}a'_{1235}m_{1235} + a_{1635}a'_{1234}m_{1234} = 0, \end{aligned} \tag{36}$$

and

$$\begin{aligned} &a_{2241}a''_{3456}m_{12} + a_{2143}a''_{2456}m_{13} + a_{2441}a''_{2356}m_{14} + a_{2145}a''_{2346}m_{15} + a_{2641}a''_{2345}m_{16} + \\ &a_{2342}a''_{1456}m_{23} + a_{2244}a''_{1356}m_{24} + a_{2542}a''_{1346}m_{25} + a_{2246}a''_{1345}m_{26} + a_{2443}a''_{1256}m_{34} \\ &+ a_{2345}a''_{1246}m_{35} + a_{2643}a''_{1245}m_{36} + a_{2544}a''_{1236}m_{45} + a_{2446}a''_{1235}m_{46} + a_{2645}a''_{1234}m_{56} = 0, \end{aligned} \tag{37}$$

where $m_{ijkl} = m_im_jm_km_l$, $m_{ij} = m_im_j$ for $i,j,k,l = 1,2,3,4,5,6$.

For short wavelengths and finite real velocity so that m_i is real, the quantity kD is very large and $\tanh x \to 1$. In this case, Eqs. (30) and (34), respectively, reduce to

$$\begin{aligned} &a_{1231}a'_{3456} + a_{1133}a'_{2456} + a_{1431}a'_{2356} + a_{1135}a'_{2346} + a_{1631}a'_{2345} + \\ &a_{1332}a'_{1456} + a_{1234}a'_{1356} + a_{1532}a'_{1346} + a_{1236}a'_{1345} + a_{1433}a'_{1256} + \\ &a_{1335}a'_{1246} + a_{1633}a'_{1245} + a_{1534}a'_{1236} + a_{1436}a'_{1235} + a_{1635}a'_{1234} = 0, \end{aligned} \tag{38}$$

and

$$\begin{aligned} &a_{2241}a''_{3456} + a_{2143}a''_{2456} + a_{2441}a''_{2356} + a_{2145}a''_{2346} + a_{2641}a''_{2345} + \\ &a_{2342}a''_{1456} + a_{2244}a''_{1356} + a_{2542}a''_{1346} + a_{2246}a''_{1345} + a_{2443}a''_{1256} + \\ &a_{2345}a''_{1246} + a_{2643}a''_{1245} + a_{2544}a''_{1236} + a_{2446}a''_{1235} + a_{2645}a''_{1234} = 0. \end{aligned} \tag{39}$$

These equations present the secular equations for Rayleigh waves in microstretch thermoelastic diffusion materials, and these results exactly match with Kumar et al. [34] for the relevant problem.

6.2 Anti-symmetric vibration

If we consider longer wavelength compared to the thickness of the plate with real m_r, then $\tanh x \to x - \frac{x^3}{3}$. Equations(31) and (35) reduce, respectively, to

$$\begin{aligned} &a_{1231}a'_{3456}r_{12}m_{12} + a_{1133}a'_{2456}r_{13}m_{13} + a_{1431}a'_{2356}r_{14}m_{14} + a_{1135}a'_{2346}r_{15}m_{15} \\ &+ a_{1631}a'_{2345}r_{16}m_{16} + a_{1332}a'_{1456}r_{23}m_{23} + a_{1234}a'_{1356}r_{24}m_{24} + a_{1532}a'_{1346}r_{25}m_{25} \\ &+ a_{1236}a'_{1345}r_{26}m_{26} + a_{1433}a'_{1256}r_{34}m_{34} + a_{1335}a'_{1246}r_{35}m_{35} + a_{1633}a'_{1245}r_{36}m_{36} \\ &+ a_{1534}a'_{1236}r_{45}m_{45} + a_{1436}a'_{1235}r_{46}m_{46} + a_{1635}a'_{1234}r_{56}m_{56} = 0, \end{aligned} \tag{40}$$

and

$$\begin{aligned}&a_{2241}a''_{3456}r_{3456}m_{3456}+a_{2143}a''_{2456}r_{2456}m_{2456}+a_{2441}a''_{2356}r_{2356}m_{2356}+a_{2145}a''_{2346}r_{2346}m_{2346}\\&+a_{2641}a''_{2345}r_{2345}m_{2345}+a_{2342}a''_{1456}r_{1456}m_{1456}+a_{2244}a''_{1356}r_{1356}m_{1356}+a_{2542}a''_{1346}r_{1346}m_{1346}\\&+a_{2246}a''_{1345}r_{1345}m_{1345}+a_{2443}a''_{1256}r_{1256}m_{1256}+a_{2345}a''_{1246}r_{1246}m_{1246}+a_{2643}a''_{1245}r_{1245}m_{1245}\\&+a_{2544}a''_{1236}r_{1236}m_{1236}+a_{2446}a''_{1235}r_{1235}m_{1235}+a_{2645}a''_{1234}r_{1234}m_{1234}=0,\end{aligned}\tag{41}$$

where $r_i = 1 - \frac{m_i^2 D^2}{3}$, $r_{ij} = r_i r_j$, $r_{ijkl} = r_i r_j r_k r_l$ for $i, j, k, l = 1, 2, 3, 4, 5, 6$.

Equations (40) and (41) give the secular equations for the flexural waves in microstretch thermoelastic diffusion plate.

7 Special cases

Case (i) In the absence of diffusion effect, the problem reduces to Lamb wave propagation in microstretch thermoelastic plate. Under this condition, d, a, α_{c1}, α_{c2}, b, τ^1 and τ^0 vanish. Consequently, $\gamma_{14} = \gamma_{24} = \gamma_{34} = 0$. The secular equations (30, 31, 34 and 35) for both symmetric and anti-symmetric cases reduce, respectively, to

$$\begin{aligned}&a_{1132}a'_{356}c_{t12}+a_{1331}a'_{256}c_{t13}+a_{1135}a'_{236}c_{t15}+a_{1631}a'_{235}c_{t16}+a_{1233}a'_{156}c_{t23}+\\&a_{1532}a'_{136}c_{t25}+a_{1236}a'_{135}c_{t26}+a_{1335}a'_{126}c_{t35}+a_{1633}a'_{125}c_{t36}+a_{1536}a'_{123}c_{t56}=0,\end{aligned}\tag{42}$$

$$\begin{aligned}&a_{1132}a'_{356}t_{12}+a_{1331}a'_{256}t_{13}+a_{1135}a'_{236}t_{15}+a_{1631}a'_{235}t_{16}+a_{1233}a'_{156}t_{23}+\\&a_{1532}a'_{136}t_{25}+a_{1236}a'_{135}t_{26}+a_{1335}a'_{126}t_{35}+a_{1633}a'_{125}t_{36}+a_{1536}a'_{123}t_{56}=0,\end{aligned}\tag{43}$$

$$\begin{aligned}&a_{2142}a''_{356}t_{12}+a_{2341}a''_{256}t_{13}+a_{2145}a''_{236}t_{15}+a_{2641}a''_{235}t_{16}+a_{2243}a''_{156}t_{23}+\\&a_{2542}a''_{136}t_{25}+a_{2246}a''_{135}t_{26}+a_{2345}a''_{126}t_{35}+a_{2643}a''_{125}t_{36}+a_{2546}a''_{123}t_{56}=0,\end{aligned}\tag{44}$$

and

$$\begin{aligned}&a_{2142}a''_{356}c_{t12}+a_{2341}a''_{256}c_{t13}+a_{2145}a''_{236}c_{t15}+a_{2641}a''_{235}c_{t16}+a_{2243}a''_{156}c_{t23}+\\&a_{2542}a''_{136}c_{t25}+a_{2246}a''_{135}c_{t26}+a_{2345}a''_{126}c_{t35}+a_{2643}a''_{125}c_{t36}+a_{2546}a''_{123}c_{t56}=0,\end{aligned}\tag{45}$$

where

$$a'_{pqr}=\begin{vmatrix}a_{2p}&a_{2q}&a_{2r}\\a_{4p}&a_{4q}&a_{4r}\\a_{5p}&a_{5q}&a_{5r}\end{vmatrix}\ \text{and}\ a''_{pqr}=\begin{vmatrix}a_{1p}&a_{1q}&a_{1r}\\a_{3p}&a_{3q}&a_{3r}\\a_{7p}&a_{7q}&a_{7r}\end{vmatrix}\ \text{for}\ p,q,r=1,2,4,5,6;$$
$$a_{jq}=a_{jr}=0\ \text{ for }\ j=5,6,7,8,\ \text{ and }\ q,r\geq 5.$$

These expressions match with the results of Kumar and Pratap [36].

Case (ii) If we neglect the microstretch, thermal and diffusion effects, the present study reduces to the propagation of Lamb wave in micropolar elastic plate. In this case, λ_0, α_0, λ_1, b_0, j_0, d, a, α_{c1}, α_{c2}, b, τ^1, τ^0, τ_1, τ_0, K^*, a, α_{t1}, α_{t2} and C^* vanish. Consequently, $\gamma_{12} = \gamma_{22} = \gamma_{32} = \gamma_{13} = \gamma_{23} = \gamma_{33} = \gamma_{14} = \gamma_{24} = \gamma_{34} = 0$. Equations (30 and 34) reduce to

$$a_{11}(a_{25}a_{36}c_{t6} - a_{26}a_{35}c_{t5})c_{t1} + a_{1635}a_{21}c_{t56} = 0. \tag{46}$$

Similarly, Equations (31 and 35) transform to

$$a_{11}(a_{25}a_{36}t_6 - a_{26}a_{35}t_5)t_1 + a_{1635}a_{21}t_{56} = 0, \tag{47}$$

where $c_{ti} = \coth(m_i D)$, and $t_i = \tanh(m_i D)$.

These results are similar to those of Kumar and Pratap [35].

Case (iii) If the micropolar and diffusion effects are neglected, then the problem reduces to the propagation of Lamb wave in a thermoelastic plate. In this case, the parameters λ_0, α_0, λ_1, b_0, j_0, j, α, β, γ, κ, β_2, ν_2, a, τ^0, τ^1, b and d vanish, and consequently, $\gamma_{13} = \gamma_{23} = \gamma_{33} = \gamma_{45} = \gamma_{14} = \gamma_{24} = \gamma_{34} = 0$. Equations (30, 31, 34 and 35), respectively, reduce to

$$a_{12}a_{25}a_{51}c_{t2} - a_{11}a_{25}a_{52}c_{t1} + a_{15}a_{2152}c_{t5} = 0, \tag{48}$$

$$a_{12}a_{25}a_{51}t_2 - a_{11}a_{25}a_{52}t_1 + a_{15}a_{2152}t_5 = 0, \tag{49}$$

$$a_{21}a_{15}a_{72}t_1 - a_{22}a_{15}a_{71}t_2 + a_{25}a_{1172}t_5 = 0, \tag{50}$$

and

$$a_{21}a_{15}a_{72}c_{t1} - a_{22}a_{15}a_{71}c_{t2} + a_{25}a_{1172}c_{t5} = 0. \tag{51}$$

These equations match with a particular case of Kumar and Pratap [36].

Case (iv) In the absence of micropolar, diffusion and thermal effects, the problem reduces to Lamb wave propagation of isotropic elastic solid. In this case, all the parameters except λ, μ and ρ vanish, and consequently, all the coupling parameters vanish. The secular equations (30, 31, 34 and 35) reduce to

$$\left[\frac{t_5}{t_1}\right]^{\pm 1} = \frac{4k^2 m_1 m_2 \mu}{(\lambda m_1^2 + 2\mu m_1^2 + \lambda k^2)(m_2^2 + k^2)}, \tag{52}$$

where $+1$ corresponds to symmetric vibration modes and -1 corresponds to anti-symmetric vibration modes. These are well-known secular equations of Rayleigh–Lamb waves in classical elasticity [28].

8 Numerical computations

We develop a program in MATLAB to compute the phase velocity and attenuation of the Lamb wave. Aluminum epoxy has wide use from electrical conduits to airplane parts, to household goods and beyond. Hence, the study of Lamb wave in the aluminum epoxy medium can be used for quick inspection of the structures built using aluminum epoxy. The following relevant parameters of aluminum epoxy [12] and thermal and diffusion parameters [14] are taken as Table 2.

Equations (17 and 18) are of the form $G(m, k) = 0$ and are solved for 'm' using the roots function of MATLAB at a fixed value of phase velocity corresponding to the longitudinal wave. These roots are taken as m_i and used in solving the secular equations. The secular equations (30, 31, 34 and 35) are solved numerically by the iteration method using 'for loop' programming for wavenumbers

Table 2 Numerical values of parameters

Parameters	Values	Parameters	Values
λ	$7.59 \times 10^9 Nm^{-2}$	μ	$1.90 \times 10^9 Nm^{-2}$
κ	$1.3234 \times 10^5 Nm^{-2}$	λ_0	$5.7702 \times 10^2 N$
λ_1	$3.4650 \times 10^4 N$	j, j_0	$1.96 \times 10^{-7} m^2$
α	$8.3255 \times 10N$	β	$1.0282 \times 10^2 N$
γ	$3.3349 \times 10^3 N$	ρ	$2192 kgm^{-3}$
α_0	$1.5947 \times 10^4 N$	C^*	$1.04 \times 10^3 Jkg^{-1}K^{-1}$
K^*	$1.7 \times 10^6 Jm^{-1}s^{-1}K^{-1}$	α_{t1}	$2.33 \times 10^{-5} K^{-1}$
α_{t2}	$2.48 \times 10^{-5} K^{-1}$	α_{c1}	$2.65 \times 10^{-4} m^3 kg^{-1}$
α_{c2}	$2.83 \times 10^{-4} m^3 kg^{-1}$	T_0	$298K$
a	$2.9 \times 10^4 m^2 s^{-2} K^{-1}$	b	$32 \times 10^5 kg^{-1} m^5 s^{-2}$
d	$0.85 \times 10^{-8} kgm^{-3} s$	b_0	$9.6 \times 10^4 N$
D	$1\ m$		

of symmetric and anti-symmetric vibrations. We have observed from Eqs. (30, 31, 34 and 35) that there exist three modes in the solution of secular equations for the symmetric and anti-symmetric vibrations in the microstretch thermoelastic diffusion plate. One of these modes is the counterpart of the classical Lamb wave and the other two modes arise due to the presence of thermo-diffusion and microstretch effects. The phase velocity and attenuation for the surface waves are defined as [13]

$$v_i = \frac{\omega}{Re(k_i)}, \qquad |A_i| = -Im(k_i), \quad (i = 1, 2, 3, 4, 5, 6).$$

The velocity curves and attenuation for symmetric and anti-symmetric vibration with angular frequency (ω) are plotted in Figs. 2, 3, 4, 5, 6, 7, 8 and 9, and a comparison for the three thermoelastic theories has been shown. We choose the following suitable values for different thermoelastic theories:

for $G - L$ theory: $\tau_0 = 0.001s$, $\tau^0 = 0.003s$, $\tau_1 = 0.009s$, $\tau^1 = 0.005s$, $\varepsilon = 0$, $\gamma_1 = 0.003s$.

for $L - S$ theory: $\tau_1 = \tau^1 = 0$, $\tau_0 = 0.001s$, $\tau^0 = 0.003s$, $\varepsilon = 1$, $\gamma_1 = 0.001s$.

for CT theory: $\tau_1 = \tau^1 = \tau_0 = \tau^0 = 0$, $\gamma_1 = 0.002s$.

Figures 2 and 3 present the velocities of three modes of symmetric and anti-symmetric vibrations for thermally insulated and impermeable plate. The velocity curves corresponding to mode-1 for both symmetric and anti-symmetric vibration in Figs. 2a and 3a, respectively, ascend with the increasing ω. The velocity corresponding to mode-2 diminishes for symmetric vibrations and enlarges for anti-symmetric vibrations as the impact of ω surges. The velocity curves represented by mode-3 for both symmetric and anti-symmetric cases in Figs. 2c and 3c lessen with ω. Figures 4 and 5 represent the attenuation of the three modes of symmetric and anti-symmetric vibrations for thermally insulated and impermeable plate. The attenuation curves

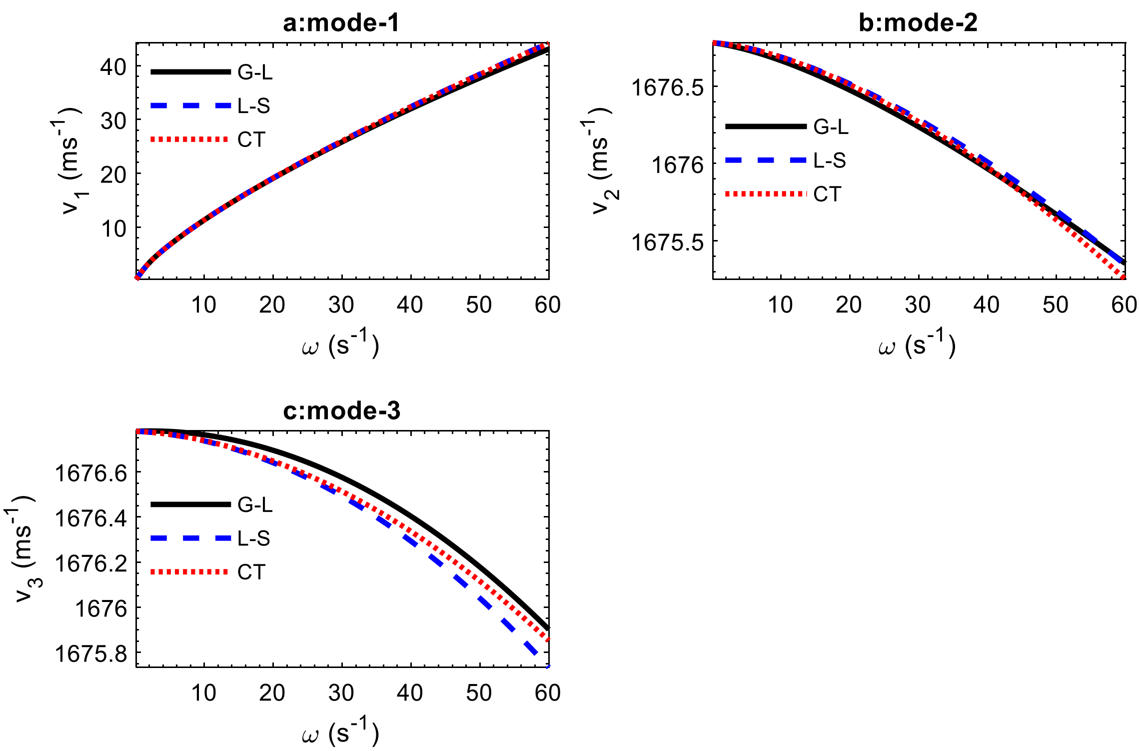

Fig. 2 Dispersion of symmetric vibrations for thermally insulated and impermeable plate

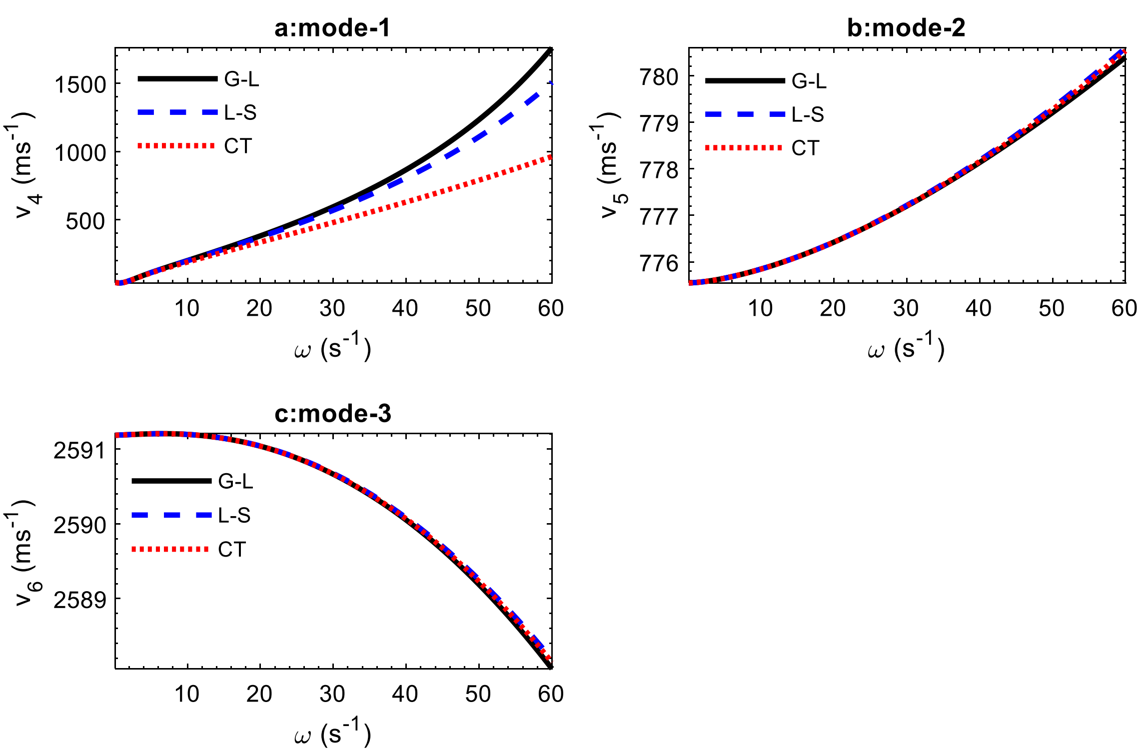

Fig. 3 Dispersion of anti-symmetric vibrations for thermally insulated and impermeable plate

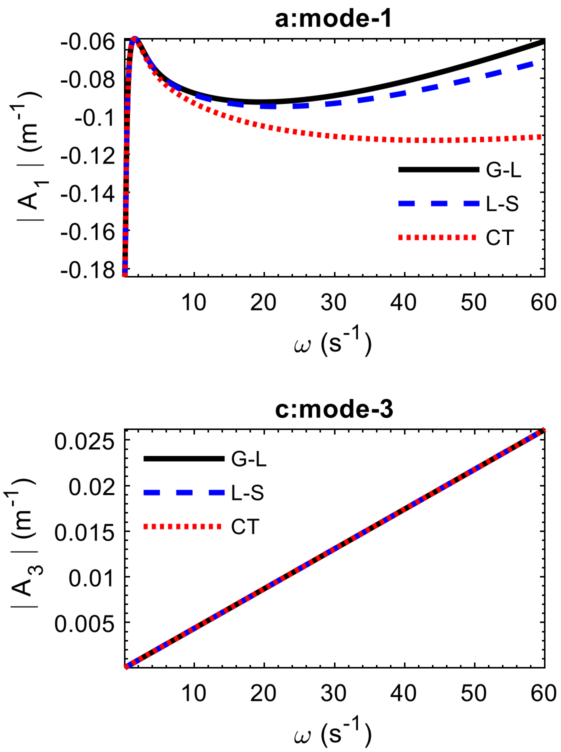

Fig. 4 Attenuation of symmetric vibrations for thermally insulated and impermeable plate

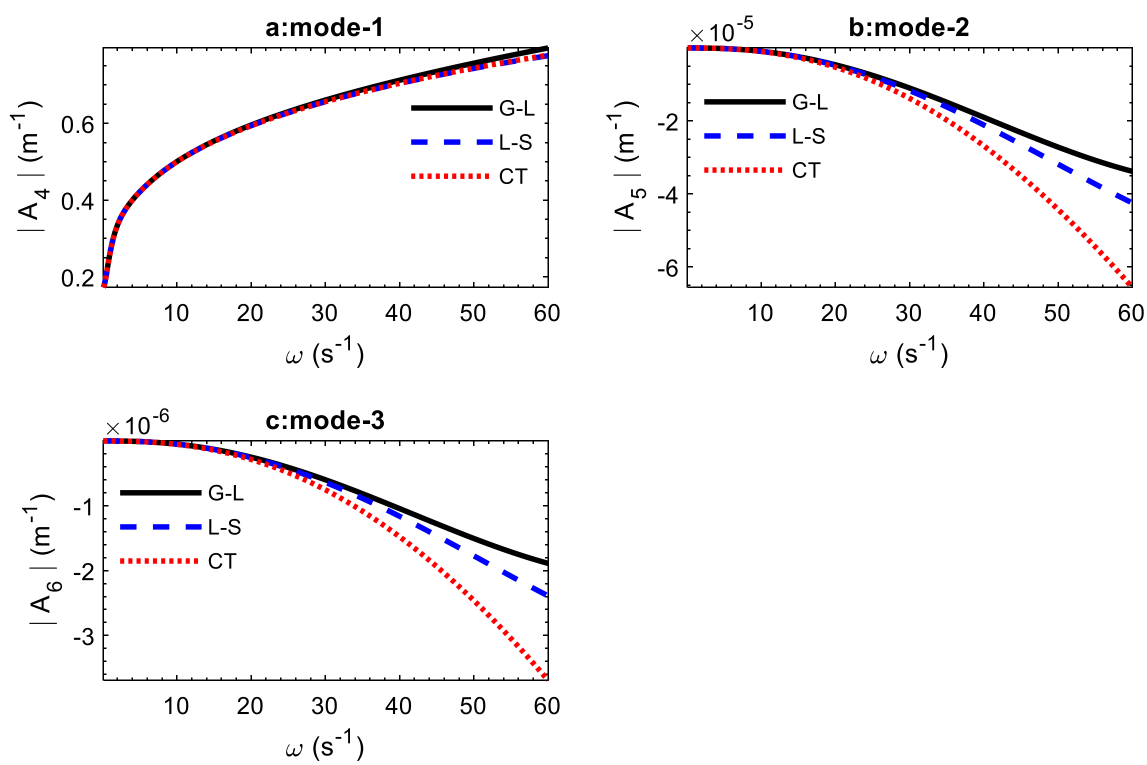

Fig. 5 Attenuation of anti-symmetric vibrations for thermally insulated and impermeable plate

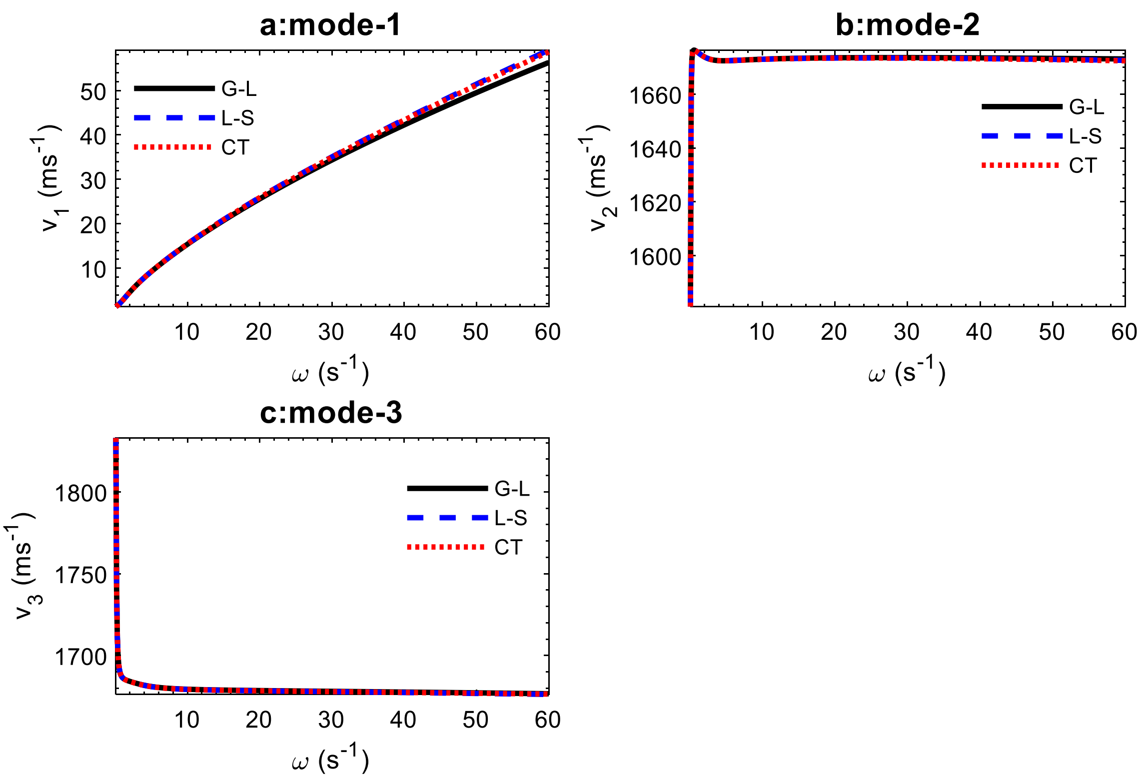

Fig. 6 Dispersion of symmetric vibrations for isothermal and isoconcentrated plate

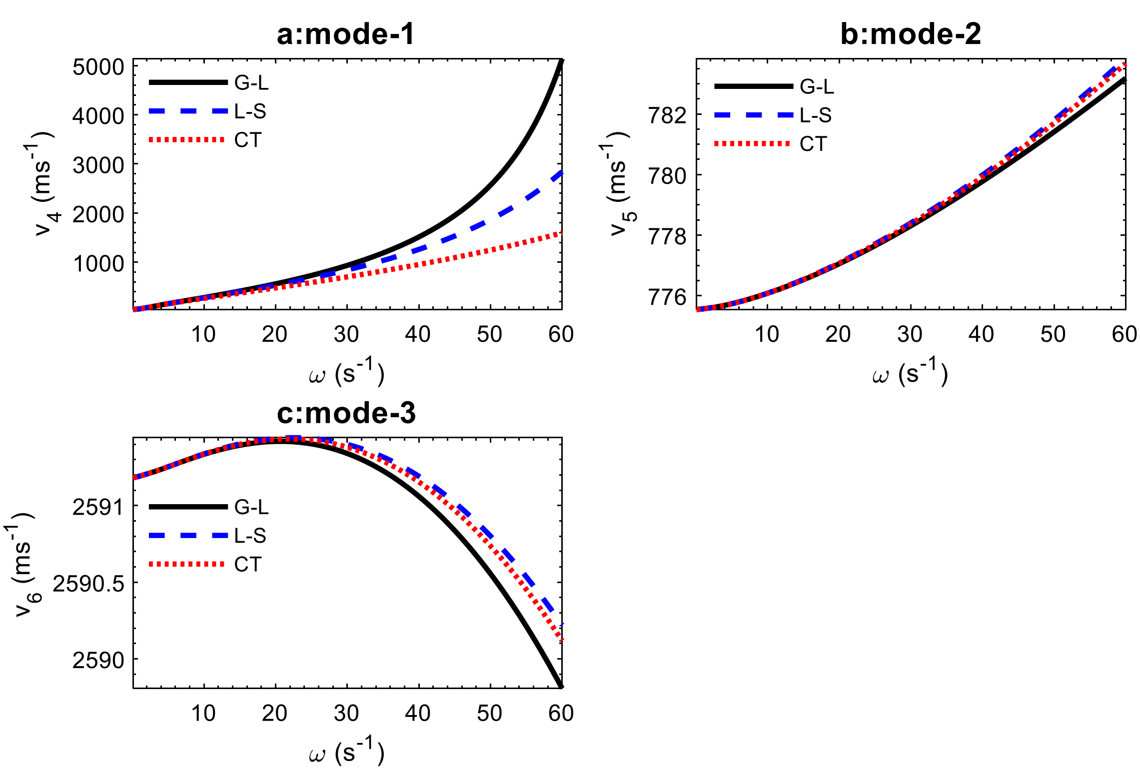

Fig. 7 Dispersion of anti-symmetric vibrations for isothermal and isoconcentrated plate

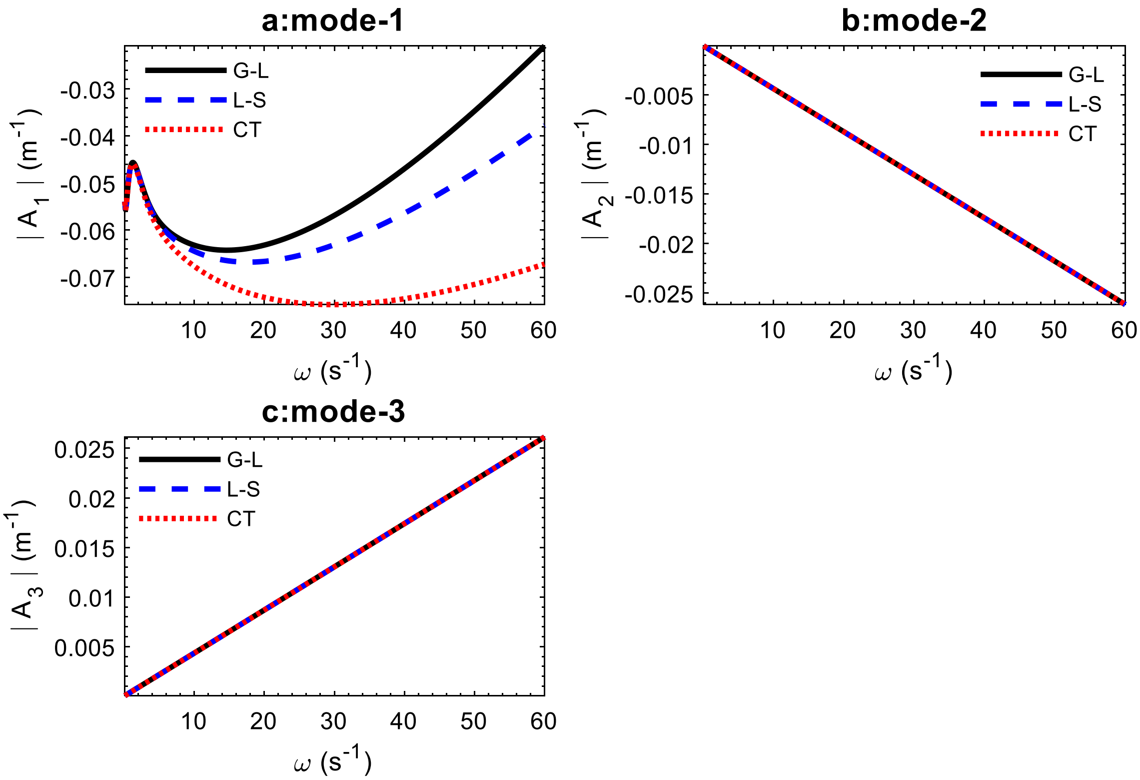

Fig. 8 Attenuation of symmetric vibrations for isothermal and isoconcentrated plate

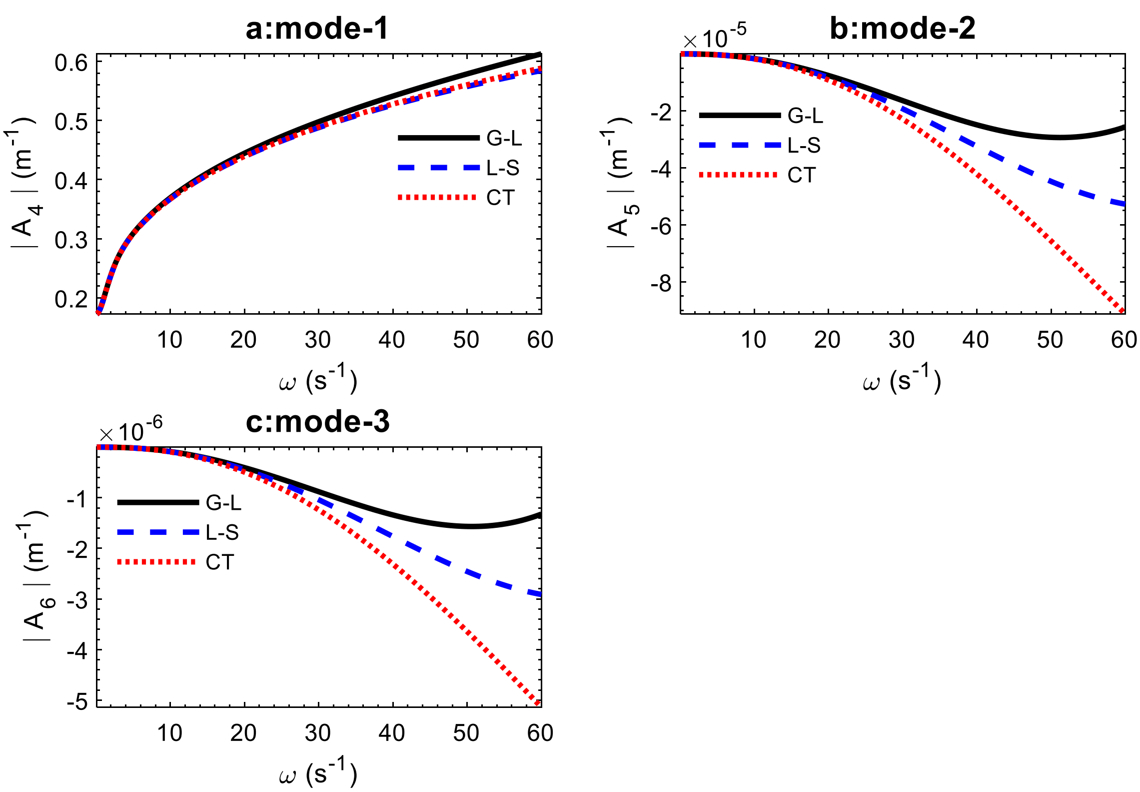

Fig. 9 Attenuation of anti-symmetric vibrations for isothermal and isoconcentrated plate

for mode-1 corresponding to anti-symmetric vibration in Fig. 5a and mode-3 corresponding to symmetric vibration in Fig. 4c escalate, while the attenuation curves in Figures 4b, 5b and c decrease with ω. The attenuation corresponding to mode-1 for symmetric vibration shoots up to $-0.5955\ ms^{-1}$ at $\omega = 1.5\ s^{-1}$ and then declines up to a certain angular frequency which increases thereafter.

Figures 6 and 7, respectively, depict the velocity of symmetric and anti-symmetric vibration for an isothermal and isoconcentrated plate. Positive effects of ω are noticed on the mode-1 velocity curves for both symmetric and anti-symmetric vibrations in Figs. 6a and 7a, while the mode-2 corresponding to anti-symmetric vibrations in Fig. 7b ascends with ω. The mode-2 velocity curve for symmetric case shoots up from $1581.0039\ ms^{-1}$ to $1675.5786\ ms^{-1}$ at $\omega = 0.4\ s^{-1}$ and sets off to a gentle descending path. The mode-3 curve for symmetric vibrations falls steeply to $1687.9793\ ms^{-1}$ at $\omega = 0.8\ s^{-1}$ and then declines gently thereafter, while the velocity curve of same mode for anti-symmetric vibration in Fig. 7c inclines for certain angular frequency and then decreases. Figures 8 and 9 represent the attenuations of symmetric and anti-symmetric vibration, respectively, for an isothermal and isoconcentrated plate. The attenuation curve represented by mode-1 of symmetric vibration elevates from $-0.055713m^{-1}$ at $\omega = 0.2s^{-1}$ to $-0.045635m^{-1}$ at $\omega = 1.3s^{-1}$ and then descends to ascend thereafter. The mode-2 attenuation for symmetric and mode-2 and mode-3 for anti-symmetric vibration decrease and mode-1 attenuation for anti-symmetric vibration and mode-3 for symmetric vibration increase with ω.

For both thermally insulated/impermeable and isothermal/isoconcentrated plates, the mode-1 velocity curve for symmetric vibration is the lowest in $G-L$ theory and same values for the other two theories, while the velocity of same mode for anti-symmetric vibration attains the highest value in the $G-L$ theory followed by $L-S$ and CT theories. The mode-3 velocity curve for symmetric vibration in Fig. 2c is highest under $G-L$ theory followed by CT and $L-S$ theories. The mode-2 and mode-3 velocity curves for symmetric vibrations in the isothermal/isoconcentrated plate coincide for all the three theories. In both the plates, the mode-2 and mode-3 velocity curves for anti-symmetric vibration acquire the highest value under the $L-S$ theory followed by CT and $G-L$ theories. The mode-1 attenuation curve for symmetric vibration and mode-2 and mode-3 for anti-symmetric vibration are highest under the $G-L$ theory followed by $L-S$ and CT theories. In the thermally insulated/impermeable and isothermal/isoconcentrated plates, the mode-2 and mode-3 attenuation curves for symmetric vibration coincide for all three theories, while the mode-1 for anti-symmetric vibration attains the highest value under $G-L$ theory and coincide for the other two theories.

9 Conclusions

The propagation of Lamb wave subject to thermally insulated/impermeable and isothermal /isoconcentrated boundary conditions in a homogeneous microstretch thermoelastic diffusion plate has been investigated. We have obtained the secular equations for symmetric and anti-symmetric vibrations in the plate. The velocity curves and attenuation of the surface waves are computed numerically for a model, and results are depicted graphically. We summarize with the following remarks:

(i) The secular equations explicate the behavior of different modes of the symmetric and anti-symmetric vibrations of Lamb wave. The secular equations corresponding to the plate waves and Rayleigh are obtained as a limiting case by considering longer and shorter wavelength, respectively.

(ii) Three modes of solution exist for the secular equation of symmetric and anti-symmetric vibrations, plate, flexural and Rayleigh waves. The phase velocity and the attenuation coefficients for all three modes depend on angular frequency, thermal, diffusion, microstretch, micropolar and Lamé parameters. The velocity of the corresponding Lamb wave increases from the first to the third mode of symmetric vibration.

(iii) In both thermally insulated/impermeable and isothermal/isoconcentrated plates, the velocity curves corresponding to mode-2 and mode-3 for anti-symmetric vibration attain the highest values under the L-S theory and followed by CT and G-L theories. The attenuations corresponding to mode-2 and mode-3 for symmetric vibration coincide for all three theories, while the attenuation of mode-1 for anti-symmetric vibration attains the highest value under G-L theory and the same results for other two theories.

Annexure - I

$$A = c_3^2c_9^2c_{15}^2c_{19}^2 - c_6^2c_9^2c_{15}^2\beta_2,$$

$$B = c_9^2c_{15}^2c_{19}^2\omega^2 + c_3^2c_9^2c_{14}^2c_{19}^2 + c_3^2c_9^2c_{15}^2c_{18}^2 + c_3^2c_9^2c_{16}^2c_{17}^2 - c_3^2c_8^2c_{15}^2c_{19}^2 + c_3^2c_{11}^2c_{15}^2\nu_2 + c_5^2c_9^2c_{12}^2c_{19}^2$$
$$+ c_5^2c_9^2c_{16}^2\beta_2 + c_4^2c_7^2c_{15}^2c_{19}^2 - c_4^2c_{11}^2c_{15}^2\beta_2 - c_6^2c_7^2c_{15}^2\nu_2 + c_6^2c_9^2c_{12}^2c_{17}^2 - c_6^2c_9^2c_{14}^2\beta_2 + c_6^2c_8^2c_{15}^2\beta_2,$$

$$C = c_9^2c_{14}^2c_{19}^2\omega^2 + c_9^2c_{15}^2c_{18}^2\omega^2 + c_9^2c_{16}^2c_{17}^2\omega^2 - c_8^2c_{15}^2c_{19}^2\omega^2 + c_{11}^2c_{15}^2\nu_2\omega^2 - c_3^2c_{10}^2c_{13}^2c_{19}^2 -$$
$$c_3^2c_{10}^2c_{16}^2\nu_2 + c_3^2c_9^2c_{14}^2c_{18}^2 - c_3^2c_8^2c_{14}^2c_{19}^2 - c_3^2c_8^2c_{15}^2c_{18}^2 - c_3^2c_8^2c_{16}^2c_{17}^2 + c_3^2c_{11}^2c_{14}^2\nu_2 - c_3^2c_{11}^2c_{13}^2c_{17}^2$$
$$+ c_5^2c_7^2c_{13}^2c_{19}^2 + c_5^2c_7^2c_{16}^2\nu_2 + c_5^2c_9^2c_{12}^2c_{18}^2 - c_5^2c_8^2c_{12}^2c_{19}^2 - c_5^2c_8^2c_{16}^2\beta_2 + c_5^2c_{11}^2c_{12}^2\nu_2 - c_5^2c_{11}^2c_{13}^2\beta_2 +$$
$$c_4^2c_7^2c_{14}^2c_{19}^2 + c_4^2c_7^2c_{15}^2c_{18}^2 + c_4^2c_7^2c_{16}^2c_{17}^2 + c_4^2c_{10}^2c_{12}^2c_{19}^2 + c_4^2c_{10}^2c_{16}^2\beta_2 + c_4^2c_{11}^2c_{12}^2c_{17}^2 - c_4^2c_{11}^2c_{14}^2\beta_2$$
$$- c_6^2c_7^2c_{14}^2\nu_2 + c_6^2c_7^2c_{13}^2c_{17}^2 - c_6^2c_{10}^2c_{12}^2\nu_2 + c_6^2c_{10}^2c_{13}^2\beta_2 - c_6^2c_8^2c_{12}^2c_{17}^2 + c_6^2c_8^2c_{14}^2\beta_2,$$

$$E = c_9^2c_{14}^2c_{18}^2\omega^2 - c_{10}^2c_{13}^2c_{19}^2\omega^2 - c_{10}^2c_{16}^2\nu_2\omega^2 - c_8^2c_{14}^2c_{19}^2\omega^2 - c_8^2c_{15}^2c_{18}^2\omega^2 - c_8^2c_{16}^2c_{17}^2\omega^2 + c_{11}^2c_{14}^2\nu_2\omega^2$$
$$- c_{11}^2c_{13}^2c_{17}^2\omega^2 - c_3^2c_{10}^2c_{13}^2c_{18}^2 - c_3^2c_8^2c_{14}^2c_{18}^2 + c_5^2c_7^2c_{13}^2c_{18}^2 - c_5^2c_8^2c_{12}^2c_{18}^2 + c_4^2c_7^2c_{14}^2c_{18}^2 + c_4^2c_{10}^2c_{12}^2c_{18}^2,$$

$$F = c_8^2c_{14}^2c_{18}^2\omega^2 + c_{10}^2c_{13}^2c_{18}^2\omega^2,$$

$$L = c_{20}^2c_{22}^2, \quad M = \omega^2c_{22}^2 + c_2^2c_{21}^2 - c_{20}^2c_{23}^2, \quad N = \omega^2c_{23}^2.$$

Annexure - II

$$P_{1i} = c_{10}^2(c_{18}^2 + c_{19}^2(m_i^2 - k^2))c_{12}^2(m_i^2 - k^2) + c_{10}^2c_{16}^2\beta_2(m_i^2 - k^2)^2 + c_7^2(c_{18}^2 + c_{19}^2(m_i^2 - k^2))$$
$$(c_{14}^2 + c_{15}^2(m_i^2 - k^2))(m_i^2 - k^2) + c_7^2c_{16}^2c_{17}^2(m_i^2 - k^2)^2 - c_{11}^2(c_{14}^2 + c_{15}^2(m_i^2 - k^2))\beta_2(m_i^2 - k^2)^2$$
$$+ c_{11}^2c_{17}^2c_{12}^2(m_i^2 - k^2)^2,$$

$$P_{2i} = -c_7^2(c_{18}^2 + c_{19}^2(m_i^2 - k^2))c_{13}^2(m_i^2 - k^2) - c_7^2c_{16}^2\nu_2(m_i^2 - k^2)^2 - (c_9^2(m_i^2 - k^2) - c_8^2)c_{16}^2$$
$$\beta_2(m_i^2 - k^2)^2 - (c_9^2(m_i^2 - k^2) - c_8^2)(c_{18}^2 + c_{19}^2(m_i^2 - k^2))c_{12}^2(m_i^2 - k^2) - c_{11}^2c_{12}^2\nu_2(m_i^2 - k^2)^2$$
$$+ c_{11}^2c_{13}^2\beta_2(m_i^2 - k^2)^2,$$

$$P_{3i} = -c_{10}^2c_{13}^2\beta_2(m_i^2 - k^2)^2 + c_{10}^2c_{12}^2\nu_2(m_i^2 - k^2)^2 + (c_9^2(m_i^2 - k^2) - c_8^2)(c_{14}^2 + c_{15}^2(m_i^2 - k^2))$$
$$\beta_2(m_i^2 - k^2)^2 - (c_9^2(m_i^2 - k^2) - c_8^2)c_{12}^2c_{17}^2(m_i^2 - k^2)^2 + c_7^2(c_{14}^2 + c_{15}^2(m_i^2 - k^2))\nu_2(m_i^2 - k^2)^2$$
$$- c_7^2c_{17}^2c_{13}^2(m_i^2 - k^2)^2,$$

$$P_i = -c_{10}^2(c_{18}^2 + c_{19}^2(m_i^2 - k^2))c_{13}^2 - c_{10}^2c_{16}^2\nu_2(m_i^2 - k^2) + (c_9^2(m_i^2 - k^2) - c_8^2)(c_{18}^2 + c_{19}^2(m_i^2 - k^2))$$
$$(c_{14}^2 + c_{15}^2(m_i^2 - k^2)) + (c_9^2(m_i^2 - k^2) - c_8^2)c_{17}^2c_{16}^2(m_i^2 - k^2) + c_{11}^2(c_{14}^2 + c_{15}^2(m_i^2 - k^2))\nu_2(m_i^2 - k^2)$$
$$- c_{11}^2c_{17}^2c_{13}^2(m_i^2 - k^2),$$

$$c_1^2 = \frac{\lambda + 2\mu}{\rho},\ c_2^2 = \frac{\kappa}{\rho},\ c_3^2 = c_1^2 + c_2^2,\ c_4^2 = \frac{\lambda_0}{\rho},\ c_5^2 = \frac{\beta_1}{\rho}(1 - \iota\tau_1\omega),\ \ c_6^2 = \frac{\beta_2}{\rho}(1 - \iota\tau^1\omega),\ c_7^2 = \frac{2\lambda_0}{\rho j_0},$$

$$c_8^2 = \omega^2 - \frac{2\lambda_1}{\rho j_0}, c_9^2 = \frac{2\alpha_0}{\rho j_0}, c_{10}^2 = \frac{2\nu_1}{\rho j_0}(1 - \iota\tau_1\omega), c_{11}^2 = \frac{2\nu_2}{\rho j_0}(1 - \iota\tau^1\omega), c_{12}^2 = \frac{\beta_1\omega T_0}{\rho}(\iota + \varepsilon\tau_0\omega),$$

$$c_{13}^2 = \frac{\nu_1 T_0\omega}{\rho}(\iota + \varepsilon\tau_0\omega),\ c_{14}^2 = \omega c^*(\iota + \tau_0\omega),\ \ c_{15}^2 = \frac{K^*}{\rho},\ c_{16}^2 = \frac{aT_0\omega}{\rho}(\iota + \gamma_1\omega),\ \ c_{17}^2 = a(1 - \iota\omega\tau_1),$$

$$c_{18}^2 = \frac{\omega}{d}(\iota + \varepsilon\omega\tau^0),\ c_{19}^2 = b(1 - \iota\omega\tau^1),\ c_{20}^2 = \frac{\mu + \kappa}{\rho},\ c_{21}^2 = \frac{\kappa}{\rho j},\ c_{22}^2 = \frac{\gamma}{\rho j},\ \ c_{23}^2 = \frac{2\kappa}{\rho j} - \omega^2.$$

Acknowledgements The author (SS Singh) acknowledges the Science and Engineering Research Board(SERB), New Delhi, for their financial support through Grant No. EMR/2017/001723 to complete this work.

Declarations

Conflict of interest The authors declare that they have no conflict of interest.

References

1. Eringen AC (1966) Linear theory of micropolar elasticity. J Math Mech 15(6):909–923
2. Eringen AC (1999) Microcontinuum field theories I: foundations and solids. Springer, New York
3. Biot M (1956) Thermoelasticity and irreversible thermodynamics. J Appl Phys 27(3):240–253. https://doi.org/10.1063/1.1722351
4. Lord HW, Shulman Y (1967) A generalized dynamical theory of thermoelasticity. J Mec Phys Solids 15(5):299–309. https://doi.org/10.1016/0022-5096(67)90024-5
5. Green AE, Lindsay KA (1972) Thermoelasticity. J Elasticity 2(1):1–7
6. Eringen AC (1990) Theory of thermo-microstretch elastic solids. Int J Engng Sci 28(12):1291–1301. https://doi.org/10.1016/0020-7225(90)90076-U
7. De Cicco S, Nappa L (2010) On the theory of thermomicrostretch elastic solids. J Therm Stresses 22(6):565–580. https://doi.org/10.1080/014957399280751
8. Ciarletta M, Scalia A (2004) Some results in linear theory of thermomicrostretch elastic solids. Meccanica 39(3):191–206. https://doi.org/10.1023/B:MECC.0000022843.48821.af
9. Sherief H, Hamza FA, Saleh HA (2004) The theory of generalized thermoelastic diffusion. Int J Eng Sci 42(5–6):591–608. https://doi.org/10.1016/j.ijengsci.2003.05.001
10. Aoudi M (2007) Uniqueness and reciprocity theorems in the theory of generalized thermoelastic diffusion. J Therm Stresses 30:665–678. https://doi.org/10.1080/01495730701212815
11. Aouadi M (2015) On thermoelastic diffusion thin plate theory. Appl Math Mech 36(5):619–632. https://doi.org/10.1007/s10483-015-1930-7
12. Khurana A, Tomar SK (2016) Wave propagation in non-local microstretch solid. Appl Math Model 40(11–12):5858–5875. https://doi.org/10.1016/j.apm.2016.01.035
13. Goyal S, Singh D, Tomar SK (2016) Rayleigh type surface waves in a swelling porous half-space. Transp Porous Media 113(1):91–109. https://doi.org/10.1007/s11242-016-0681-3
14. Kumar R (2015) Wave propagation in a microstretch thermoelastic diffusion solid. An St ale Univ Ovidius Const 23(1):127–170. https://doi.org/10.1515/auom-2015-0010
15. Kumar R, Ahuja S, Garg S (2014) Surface wave propagation in a microstretch thermoelastic diffusion material under an inviscid liquid layer. Adv Acoust Vib 2014:1–11. https://doi.org/10.1155/2014/518384
16. Singh SS, Debnath S, Othman MIA (2022) Thermoelastic theories on the refracted waves in microstretch thermoelastic diffusion media. Int J Appl Mech 14(2):1–30
17. Royer D, Dieulesaint E (1999) Elastic waves in solids I: free and guided propagation. Springer, New York
18. Singh SS (2013) Transverse wave at a plane interface in thermoelastic materials with voids. Meccanica 48(3):617–630. https://doi.org/10.1007/s11012-012-9619-1
19. Zorammuana C, Singh SS (2016) Elastic waves in thermoelastic saturated porous medium. Meccanica 51(3):593–609. https://doi.org/10.1007/s11012-015-0225-x
20. Singh SS, Lianngenga R (2017) Effect of micro-inertia in the propagation of waves in micropolar thermoelastic materials with voids. Appl Math Model 49:487–497. https://doi.org/10.1016/j.apm.2017.05.008
21. Lofty K, Othman MIA (2012) Effect of rotation on plane waves in generalized thermo-microstretch elastic solid with a relaxation time. Meccanica 47(6):1467–1486. https://doi.org/10.1007/s11012-011-9529-7
22. Singh SS, Tochhawng L (2019) Stoneley and Rayleigh waves in thermoelastic materials with voids. J Vib Control 25(14):2053–2062. https://doi.org/10.1177/1077546319847850
23. Kumar R, Kansal T (2008) Propagation of Lamb waves in transversely isotropic thermoelastic diffusive plate. Int J Solids Struct 45(22–23):5890–5913. https://doi.org/10.1016/j.ijsolstr.2008.07.005
24. Abo-Dahab SM, Abd-Alla AM, Alsharif A, Alotaibi H (2022) On generalized waves reflection in a micropolar thermodiffusion elastic half-space under initial stress and electromagnetic field. Mech Based Des Struct Mach 50(8):2670–2687. https://doi.org/10.1080/15397734.2020.1784200
25. Kumar R, Devi S, Abo-Dahab SM (2018) Stoneley waves at the boundary surface of modified couple stress generalized thermoelastic with mass diffusion. J Appl Sci Eng 21(1):1–8. https://doi.org/10.6180/jase.201803_21(1).0001
26. Kumar R, Abo-Dahab SM, Devi S (2018) Rayleigh waves at the boundary surface of modified couple stress generalized thermoelastic with mass diffusion. Adv Compos Mater 27(3):309–329. https://doi.org/10.1080/09243046.2017.1384182
27. Singh B, Yadav AK (2021) The effect of diffusion on propagation and reflection of waves in a thermo-microstretch solid half-space. Comput Math Model 32(2):221–234. https://doi.org/10.1007/s10598-021-09527-w
28. Lamb H (1917) On waves in an elastic plate. Proc R Soc Lond A Math Phys Eng Sci 93(648):114–128
29. Zhu Z, Wu J (1995) The propagation of Lamb waves in a plate bordered with a viscous liquid. J Acoust Soc Am 98(2):1057–1064. https://doi.org/10.1121/1.413671
30. Conry M, Crane L, Gilchrist M (2000) Detection of defects in a plate using Rayleigh-Lamb waves. ZAMM 80(S2):465–466
31. Tomar SK (2005) Wave propagation in a micropolar elastic plate with voids. J Vib Control 11(6):849–863. https://doi.org/10.1177/1077546305054
32. Lianngenga R, Singh SS (2019) Symmetric and anti-symmetric vibrations in micropolar thermoelastic materials plate with voids. Appl Math Model 76:856–866. https://doi.org/10.1016/j.apm.2019.07.012
33. Sharma JN, Pal M (2004) Propagation of Lamb waves in a transversely isotropic piezothermoelastic plate. J Sound Vib 270(4–5):587–610. https://doi.org/10.1016/S0022-460X(03)00093-2
34. Kumar R, Ahuja S, Garg SK (2014) Rayleigh waves in isotropic microstretch thermoelastic diffusion solid half space. Lat Am J Solids Struct 11:299–319. https://doi.org/10.1590/S1679-78252014000200009
35. Kumar R, Partap G (2006) Rayleigh Lamb waves in micropolar isotropic elastic plate. Appl Math Mech 27(8):1049–1059. https://doi.org/10.1007/s10483-006-0805-z
36. Kumar R, Partap G (2009) Analysis of free vibrations for Rayleigh-Lamb waves in a microstretch thermoelastic plate with two relaxation times. J Eng Phys Thermophys 82:35–46. https://doi.org/10.1007/s10891-009-0170-4

37. Sharma JN, Thakur MD (2006) Effect of rotation on Rayleigh-Lamb waves in magneto-thermoelastic media. J Sound Vib 296(4–5):871–887. https://doi.org/10.1016/j.jsv.2006.03.014
38. Sharma JN, Othman MIA (2007) Effect of rotation on generalized thermo-viscoelastic Rayleigh-Lamb waves. Int J Solids Struct 44(13):4243–4255. https://doi.org/10.1016/j.ijsolstr.2006.11.016
39. Sharma JN, Kumar S (2009) Lamb waves in micropolar thermoelastic solid plates immersed in liquid with varying temperature. Meccanica 44(3):305–319. https://doi.org/10.1007/s11012-008-9170-2
40. Apostol BF (2020) On the Lamb problem: forced vibrations in a homogeneous and isotropic elastic half-space. Arch Appl Mech 90(10):2335–2346. https://doi.org/10.1007/s00419-020-01724-0
41. Ezzin H, Wang B, Qian Z, Arefi M (2021) Multiple crossing points of Lamb wave propagating in a magneto-electro-elastic composite plate. Arch Appl Mech 91:2781–2793. https://doi.org/10.1007/s00419-021-01927-z
42. Sharma V, Kumar S (2014) Velocity dispersion in an elastic plate with microstructure: effects of characteristic length in a couple stress model. Meccanica 49(5):1083–1090. https://doi.org/10.1007/s11012-013-9854-0
43. Goldstein R, Kuznetsov SV (2017) Long-wave asymptotics of Lamb waves. Mech Solids 52(6):700–707. https://doi.org/10.3103/S0025654417060097
44. Staszewski WJ, Lee BC, Mallet L, Scarpa F (2004) Structural health monitoring using scanning laser vibrometry:II. Lamb waves for damage detection. Smart Mater Struct 13(2):251–260. https://doi.org/10.1088/0964-1726/13/2/002
45. Mazzotti M, Kohtanen E, Erturk A, Ruzzene M (2021) Radiation characteristics of cranial leaky Lamb waves. IEEE Trans Ultrason Ferroelectr Freq Control 68(6):2129–2140. https://doi.org/10.1109/TUFFC.2021.3057309
46. Chen Z, Fan L, Zhang S, Zhang H (2014) Theoretical research on ultrasonic sensors based on high-order Lamb waves. J Appl Phys 115(20):504–513. https://doi.org/10.1063/1.4880335
47. Mozaffarzadeh M, Minonzio C, Jong N, Verweji MD, Hemm S, Daeichin V (2021) Lamb waves and adaptive beamforming for aberration correction in medical ultrasound imaging. IEEE Trans Ultrason Ferroelectr Freq Control 68(6):84–91. https://doi.org/10.1109/TUFFC.2020.3007345
48. Su Z, Ye L (2009) Identification of damage using lamb waves: from fundamentals to applications. Springer, Berlin

Publisher's Note Springer Nature remains neutral with regard to jurisdictional claims in published maps and institutional affiliations.